J Sol-Gel Sci Technol (2016) 80:208–214
DOI 10.1007/s10971-016-4076-2

ORIGINAL PAPER: SOL-GEL AND HYBRID MATERIALS WITH SURFACE MODIFICATION FOR APPLICATIONS

Facile fabrication of superhydrophobic silica coatings with excellent corrosion resistance and liquid marbles

Jian Li[1] · Zhihong Zhao[1] · Yan Zhang[1] · Bin Xiang[1] · Xiaohua Tang[1] · Houde She[1]

Received: 29 February 2016 / Accepted: 13 May 2016 / Published online: 20 May 2016

Abstract Self-cleaning superhydrophobic coatings with water contact angle as high as 156° and sliding angle as low as 3° were prepared through a facile one-step spray coating process by spraying the hydrophobic silica nanoparticles onto Al substrate. In addition, the superhydrophobic coatings maintained excellent electrochemical corrosion resistance in a 3.5 wt% NaCl aqueous solution. The corrosion behavior of the superhydrophobic coatings on the Al substrate was characterized by the polarization curve and electrochemical impedance spectroscopy. The results indicated that the superhydrophobic coatings possessed excellent corrosion resistance. In addition, liquid marbles coated with hydrophobic silica nanoparticles were prepared by gentle rolling of liquid on powder beds of hydrophobic silica nanoparticles. Furthermore, water evaporation from the silica shell with time evolution was investigated using a contact angle measurement system video camera.

Graphical Abstract Superhydrophobic silica surface with excellent corrosion resistance and liquid marbles coated with hydrophobic silica were fabricated by a facile process.

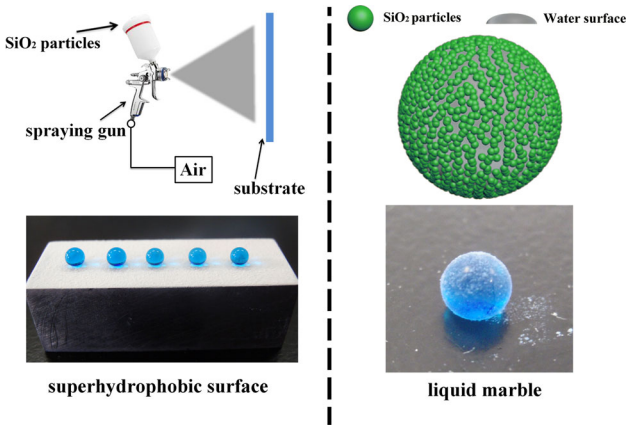

Keywords Superhydrophobic · Liquid marbles · Silica nanoparticles · Corrosion resistance · Spray coating

1 Introduction

In nature, many surfaces are superhydrophobic possessing apparent water contact angle (CA) >150° and low contact angle hysteresis (CAH). The best example is lotus leaf with high contact angle and low hysteresis, which is attributed to the cooperative effect of the hydrophobic waxy and the hierarchical rough surface [1]. To obtain a superhydrophobic surface, two traditional conditions must be attained: a hierarchical roughness and low surface energy [2]. Superhydrophobic materials were widely applied in various aspects during the last few decades, such as in self-cleaning [3], transparent coatings [4, 5], anticorrosion [6], oil/water separation [7–9] and selective transportation of microdroplets [10]. Metal is widely applied in the modern society, so the corrosion of the metal received considerable

Electronic supplementary material The online version of this article (doi:10.1007/s10971-016-4076-2) contains supplementary material, which is available to authorized users.

✉ Jian Li
jianli83@126.com

[1] Key Laboratory of Eco-Environment-Related Polymer Materials, Ministry of Education of China, Key Laboratory of Gansu Polymer Materials, College of Chemistry and Chemical Engineering, Northwest Normal University, Lanzhou 730070, China

attention. Superhydrophobic performance is very advantageous for the anticorrosion of the metal, and many methods have been proposed to fabricate the superhydrophobic film on all kinds of metal surfaces such as Cu, Al and Zn [11]. These methods mainly include chemical etching [12], anodization [13], electrodeposition [14], spraying method [15, 16], etc. The one-step spraying method is a fairly facile and commercially available method for the widest applications, which is not specific to a particular substrate and can be easily applied to large surface area [17]. Herein, the superhydrophobic surfaces are fabricated using a facile one-step process by spraying the hydrophobic silica nanoparticles that were synthesized by sol–gel method and modified with octadecyltrichlorosilane (OTS). The hydrophobic silica can be used on various substrates such as paper [18], wood [19], glass [20] and fiberglass cloth [21].

Liquid marbles are nonstick droplets encapsulated with micro- or nanoscaled solid particles. Since liquid marbles were introduced in the pioneering works of Quéré et al. [22], they have been exposed to intensive theoretical and experimental research. Liquid marbles are non-wetting liquid droplets encapsulated by highly hydrophobic particles and can sit on the surface of a solid or a liquid. These hydrophobic powders spontaneously migrate to the water–air interface forming liquid marbles, which act as microreservoirs of liquid capable of moving quickly without any leakage. Due to hydrophobic powders at the liquid–air interface, the wetting between the substrate and the water is avoided. Because of the peculiar characteristics, liquid marbles have potential application in many fields, such as liquid storage [23], microreactors [24], pollution detection [25] and gas sensors [26]. The stability of liquid marbles is an important limiting factor for its application, so stability studies of liquid marbles is crucial. Water evaporation from the shell with time was used to describe the stability of liquid marbles.

The formation of superhydrophobic materials via the polymerization of OTS has been widely used [27, 28]. In our work, SiO_2 nanoparticles were successfully synthesized by sol–gel method and modified with OTS. The superhydrophobic surfaces were fabricated using a facile one-step process by spraying the hydrophobic silica nanoparticles onto Al substrate. The corrosion behavior of the superhydrophobic silica coatings on the Al substrate was also studied by the polarization curve and electrochemical impedance spectroscopy (EIS), which exhibit that the superhydrophobic coatings possess outstanding corrosion resistance. In addition, liquid marble was obtained by rolling a water drop (10 μL) over hydrophobic silica nanopowder beds. Furthermore, water evaporation from the silica shell with time evolution was investigated using a contact angle measurement system video camera.

2 Experimental

2.1 Materials

Octadecyltrichlorosilane (OTS) was obtained from Shanghai Boer Chemical Reagent Co., Ltd. Ammonia and tetraethoxysilane (TEOS) were purchased from Tianjin Kaixin Chemical Reagent Co., Ltd. Acetone, toluene and ethanol were purchased from Sinopharm Chemical Reagents and used as received. Al substrate was obtained from a local store and cleaned with acetone and ethanol before use.

2.2 Preparation of SiO_2 nanoparticles by sol–gel method

Silica nanoparticles were synthesized according to the well-known Stöber method [29]. TEOS was dispersed in the miscible liquids of anhydrous ethanol, deionized water and ammonia solution, which molar ratio was 1:37.87:3.22:0.09. The clear solution was stirred at room temperature for 2 h in a closed glass container and then aged at room temperature for 3 days. Spherical silica particles were obtained, with the diameter being about 50 ± 10 nm (see supporting information Figure S1). Finally, silica nanoparticles were then dried at room temperature.

2.3 Preparation of superhydrophobic SiO_2 nanoparticles

1 g SiO_2 nanoparticles and 40 mL toluene were placed into a round-bottom flask, and then, 1 mL of OTS was added into the solution and refluxed for 3 h. After filtration, the obtained SiO_2 nanoparticles were dried at 353 K and ground to a fine powder using a mortar; then, superhydrophobic SiO_2 nanoparticles were successfully prepared (see supporting information Figure S2).

2.4 Preparation of the superhydrophobic silica coatings on Al substrate

Silica particles (0.9 g) were dispersed in 60 mL of ethanol to obtain uniform suspensions under magnetic stirring for 1 h, and then, 0.05 g waterborne polyurethane (PU) was dispersed in the solution. Subsequently, the resulting suspensions were sprayed onto stainless Al substrate with a 0.2 MPa compressed air gas using a spray gun connected to an air compressor. The distance between the spray gun and the substrate was about 15 cm. Finally, the coatings were dried at ambient temperature for 1 h to evaporate the ethanol completely.

2.5 Preparation of silica liquid marbles

Water droplets were placed in the hydrophobic silica powder beds with a microliter syringe (10 μL). By gently rolling the aqueous droplet on the powder beds, the liquid was encapsulated by the silica powders. Finally, liquid marbles were transferred to glass sheet on the workbench of the contact angle measurement system.

2.6 Characterization

Fourier transform infrared (FT-IR) spectra were recorded on a Bio-Rad FTS-165 instrument using KBr as the background. The IR transmission spectrum were collected by pressing the particles in a KBr pellet and scanning 32 cycles from 400 to 4000 cm^{-1} at 2 cm^{-1} resolution. The morphological structure of the as-prepared surface was examined by field emission scanning electron microscopy (FE-SEM, JSM-6701F). Samples were pre-coated with a thin layer of platinum or gold, respectively, to prevent charging. Contact angle and sliding angle measurements were performed using a SL200KB apparatus at ambient temperature. The static contact angles (CAs) were measured in sessile drop mode. The sliding angles (SAs) were measured by a tilting stage method. The sliding angle is defined as the tilt angle of the stage upon which a water droplet rolls off of the surface. The as-prepared SiO_2 were also characterized by an X-ray diffractometer (XRD) (Rigaku Corp., D/max-2400) equipped with the graphite monochromatized Cu Kα radiation. About 5 mg of samples was packed into a standard cavity mount. Digital data were obtained for a 2θ range of 5°–70° at an angular resolution of 0.02° with a total counting time of 4 h.

Electrochemical measurements were measured in a 3.5 wt% NaCl corrosive solution at room temperature using a computer-controlled CHI660E electrochemical workstation, which was equipped with a three-electrode system with a saturated Ag/AgCl reference electrode, a platinum electrode as the counter electrode and the samples (bare Al film and superhydrophobic coating formed on the Al film) as the working electrode. The surface area of the test samples open to the corrosive solution was about 1 cm^2. The superhydrophobic coatings formed on the Al film were immersed in a 3.5 wt% NaCl corrosive solution to establish the open-circuit potential (E_{ocp}). The polarization curves were obtained at a sweep rate of 5 mV s^{-1}. The electrochemical impedance spectroscopy (EIS) was conducted at E_{ocp} in the frequency ranged from 10 to 100 kHz using an ac perturbation of 5 mV. Two-dimensional (2D) image of the liquid marble was obtained by an OLYMPUS-IX51 digital microscope. The water evaporation from the silica shell was characterized using the SL200KB apparatus.

3 Results and discussion

The hydrophobic SiO_2 nanoparticles were a key part of our strategy for the fabrication of superhydrophobic surfaces. From the supporting information Figure S3, it can be obtained that the as-prepared SiO_2 shows amorphous structure. Superhydrophobic silica coatings were fabricated by the subsequent introduction of the roughness surface and low surface energy through spraying the hydrophobic silica nanoparticles on the Al substrate. Figure 1a exhibits the low-magnification FE-SEM image revealing that the surface is not smooth. The surface roughness structure is established by a large number of agglomerated particles. As shown in Fig. 1b, there are also numerous irregular void spaces among individual particles. The agglomerated particles and the irregular void space led to the roughness surface. Trapped air in irregular void space is important for superhydrophobic. Therefore, this surface morphology is advantageous in bringing about excellent superhydrophobic and low adhesive properties with a CA as high as 156° ± 1° and an SA as low as 3° (Fig. 1a, b insert).

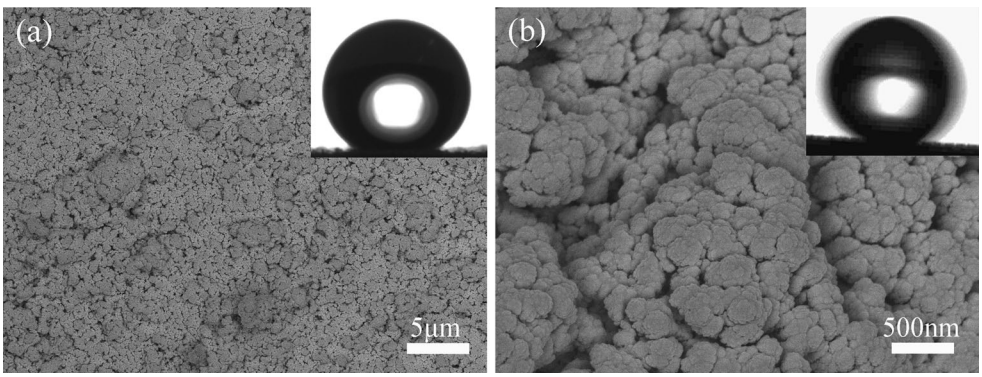

Fig. 1 **a**, **b** FE-SEM images of the as-prepared superhydrophobic coatings at low and high magnification, respectively. The *insets* show the water droplet on the coating surface with **a** a CA of 156° ± 1° and **b** a SA of 3°

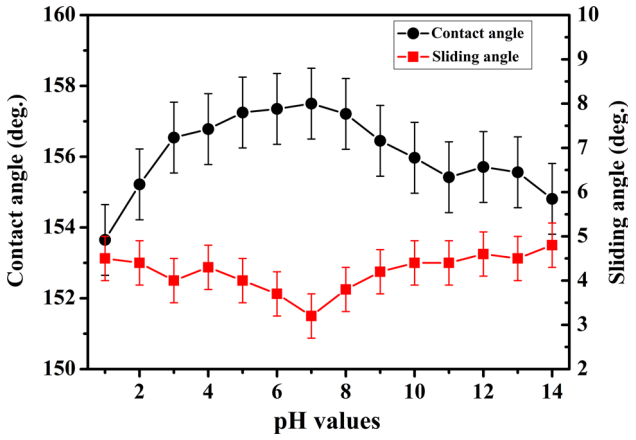

Fig. 2 Variation in the water CAs and SAs of the as-prepared superhydrophobic silica surface as a function of pH values of water droplets

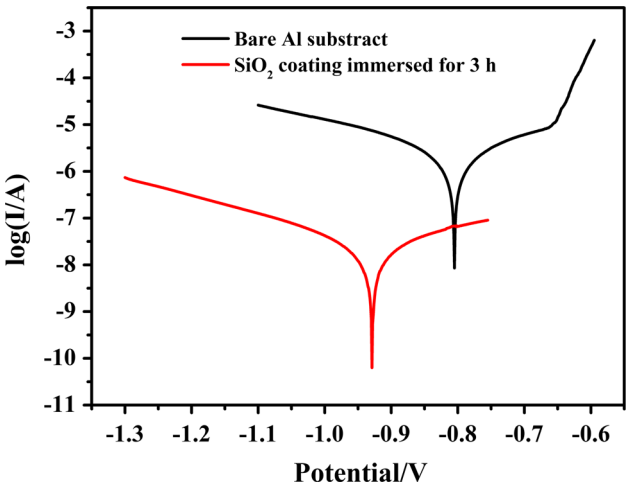

Fig. 3 Polarization curves of the bare Al substrate and superhydrophobic silica surface immersed in the 3.5 wt% NaCl solution

The chemical stability of coatings is important in practical application. The superhydrophobic silica coatings always exhibit chemical stability in different corrosive conditions. Figure 2 shows the relationship between the water CAs and SAs on the superhydrophobic silica coatings and pH values of a water droplet. As shown in Fig. 2, CA values are >150° and remain almost invariable within experimental error at all pH values of the water droplet, ranging from 1 to 14. SA values always remain below 5°, which shows the low adhesion of the as-prepared superhydrophobic silica coatings. We conclude that the superhydrophobic coatings show good chemical stability to acid droplets, basic droplets and some salt aqueous solutions.

The corrosion resistance of the superhydrophobic surfaces is a key determinant in the superhydrophobic surfaces practical applications. The corrosion resistance of the superhydrophobic silica coatings was tested in a 3.5 wt% NaCl aqueous solution by electrochemical workstation. Figure 3 shows potentiodynamic polarization curves of a bare Al substrate after immersion in the 3.5 wt% NaCl aqueous solution and the superhydrophobic silica coatings formed on an Al substrate after immersion in the 3.5 wt% NaCl aqueous solution for 3 h at room temperature. As given in Table 1, the electrochemical parameters of the corrosion current density (I_{corr}) for bare Al and the silica coatings were obtained using the Tafel extrapolation from the potentiodynamic polarization curves. It should be noted that I_{corr} of the superhydrophobic coatings on the Al substrate immersed in a 3.5 wt% NaCl corrosive solution for 3 h decreased by 2 orders of magnitude compared to that of the bare Al substrate. In a typical polarization curve, a lower corrosion current density usually indicates a lower corrosion rate and a better corrosion resistance [30, 31]. The superhydrophobic coatings on the Al substrate provide very effective protection of Al from corrosion. The surface

Table 1 E_{corr} and I_{corr} for a bare Al substrate immersed for 2 h and a SiO_2 coating immersed for 3 h were obtained from the Tafel in a 3.5 wt% NaCl solution

Sample	Bare Al	Immersed for 3 h
E_{corr} (V)	−0.805	−0.932
I_{corr} (A cm^{-2})	2.416×10^{-6}	2.42×10^{-8}

composed of some particles agglomerate and interval was appropriate for Cassie's state with a mass of trapped air [32, 33]. Studies have shown that the air was the most important element for corrosion resistance. Thus, we could conclude from analysis of Fig. 3 that the superhydrophobic coatings are effective for improving the corrosion resistance of the Al surface.

EIS is an effective and revealing method for the corrosion characterization of coated metals. In our study, the EIS measurements were performed under open-circuit potential in 3.5 wt% NaCl corrosive solutions under a working frequency range from 10 mHz to 100 kHz using an ac perturbation of 5 mV. Figure 4 presents the evolution of the impedance spectra of the superhydrophobic silica coatings formed on an Al surface after immersion in a 3.5 wt% NaCl solution for 3 h and bare Al for 2 h. Figure 4a shows that the Nyquist plot of bare Al is composed of a capacitive loop at high frequency range and a straight line in low frequency range. As shown in Fig. 4a, the superhydrophobic coatings have bigger loops than the bare Al substrate. The diameter size of capacitive loops represents the stand or fall of anticorrosion. The capacitive loops are from the trapped air, and the line presents a diffusion process [34, 35]. The conclusion which is consistent with the result forms the Bode plot of impedance modulus |Z| as a function of frequency in Fig. 4b. The impedance modulus

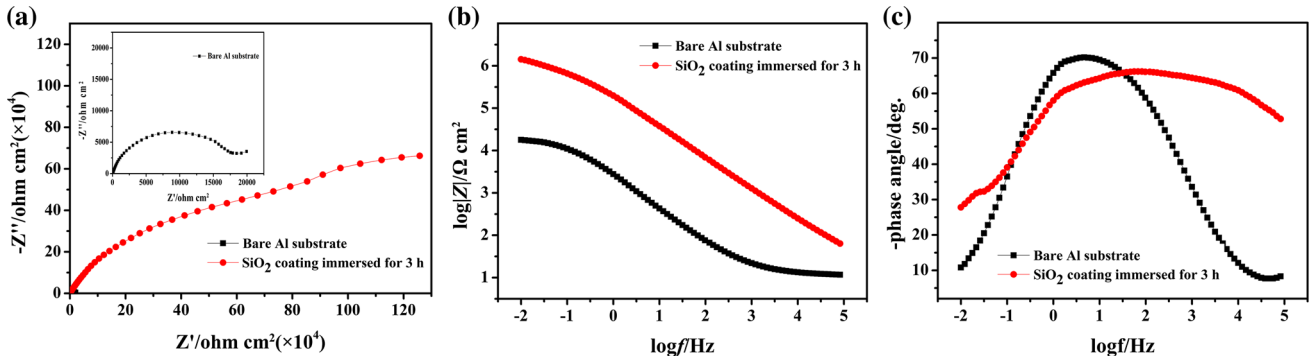

Fig. 4 EIS results of bare and the as-prepared superhydrophobic silica coatings formed on the Al surfaces in 3.5 wt% NaCl solution. **a** Nyquist plots, **b** Bode |Z| versus frequency plots and **c** Bode phase angle versus frequency plots

|Z| of the superhydrophobic coatings after immersion for 3 h at low frequency maintains a high value and is estimated to be about $1.4 \times 10^6\ \Omega\ cm^2$ (Fig. 4b). The as-prepared superhydrophobic coating immersed for 3 h is 2 orders of magnitude greater than that of the pristine Al substrate. It is well known that higher Z modulus at lower frequency displays a better corrosion resistance on the metal substrate [36, 37]. From Fig. 4c, the phenomenon of the peak value of bode phase angle diagrams moving to high frequency was obtained, indicating that superhydrophobic coatings can effectively reduce the corrosion rate of the Al. In addition, the high phase angles at the high frequency domain equally indicate the good repellent property [38, 39]. These consistent results from polarization curves and EIS further prove that the as-prepared superhydrophobic coatings formed on Al possess better corrosion resistance than bare Al. The excellent anticorrosion property of the superhydrophobic coatings should be attributed to the synergistic action of the superhydrophobic property based on the silica coatings and air trapped in the porous structure.

Lotus leaves can always keep a clean appearance despite in a mire environment in nature [40]. Studies had found that the cooperation between hierarchical structure and epicuticular wax on the leaves surface contributed to a high CA and a low SA. So water droplets can roll off instead of sliding on the surface and take away the dirt adhered on its surface effectively. Self-cleaning properties tests showed the water droplets could clean away attapulgite powder on the silica superhydrophobic coatings surface (Fig. 5). This suggests that the dispensed water droplet can collect the dust powders easily and perfectly during rolling off the surface due to the superior superhydrophobic property of the as-prepared surface. The main reason in the removal of dirt from a roughened surface is the reduction in solid/solid interfacial area for the particles sit on top of small-scale roughness without strongly constraint. Thus, the as-prepared superhydrophobic surface has an excellent function of self-cleaning.

Scratch tests were reported to be effective methods to evaluate the robustness of the superhydrophobic surface against mechanical forces [41, 42]. In our study, similar scratch tests were carried out using 800 mesh SiC sandpaper as an abrasion surface with the as-prepared superhydrophobic surface facing the abrasion material, as shown in Fig. 6a. Simultaneously, the as-prepared sample was subjected to a 5 g weight and was dragged forward and backward with a speed and abrasion length of about 2 cm s^{-1} and 5 cm, respectively. Figure 6b displays the change in the water CA as a function of scratch cycles. The results show that the water CA was still close to 150° after 80 scratch cycles. These results display that the as-prepared superhydrophobic surface has good mechanical abrasion resistance.

Furthermore, when the hydrophobic SiO_2 is in contact with a water droplet, it is picked up by the droplet and

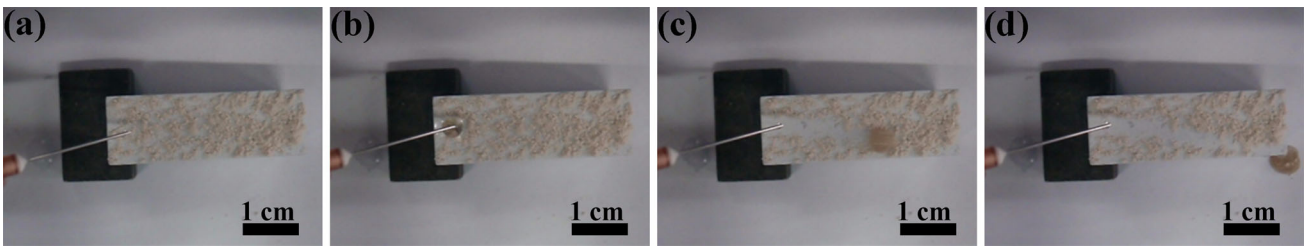

Fig. 5 Time sequence of the self-cleaning process on the superhydrophobic surface at a sliding angle about 3°

forms a porous shell around it. The Young–Dupré equation ($\Delta F = -\pi R_S^2 \gamma_{LV}(1 + \sin\theta_e)^2$ where R_S is the radius of the SiO_2, θ_e is the intrinsic contact angle, ΔF is the net change in surface free energy and γ_{LV} is the liquid–vapor interfacial tensions) suggests that it is always favorable for particle to spontaneously attach to the liquid–vapor interface, even if they are hydrophobic [43]. Figure 7a shows the 2D digital image of the liquid marble constructed by hydrophobic silica. We can observe that the silica particles are random and close-packed over water surface and there are a mass of voids between microspheres. The presence of voids areas makes the inner water can evaporate and result in the instability of liquid marbles. Meanwhile, liquid marbles with porous appearance do not wet contact substrate because of gas film existed in porous construction. Figure 7b is the illustration image of liquid marbles enwrapped by the hydrophobic silica, which are aggregated over the whole water drop surface.

The robustness of the liquid marble was measured by evaporation rate of inner water at ambient temperature. As shown in Fig. 8, the volume of the liquid marble was measured by the contact angle measurement system video camera until the liquid marble collapse completely at room temperature (35 % relative humidity, 28 °C). The state of the liquid marble was recorded every 20 min. Time evolution of a 10 μL water marble at room temperature is shown in Fig. 8a–f. Initially, the liquid marble was nearly spherical, and height of the marble started decreasing because of evaporation before 60 min, and buckling of the marble occurred in Fig. 8d. Finally, in 100 min water

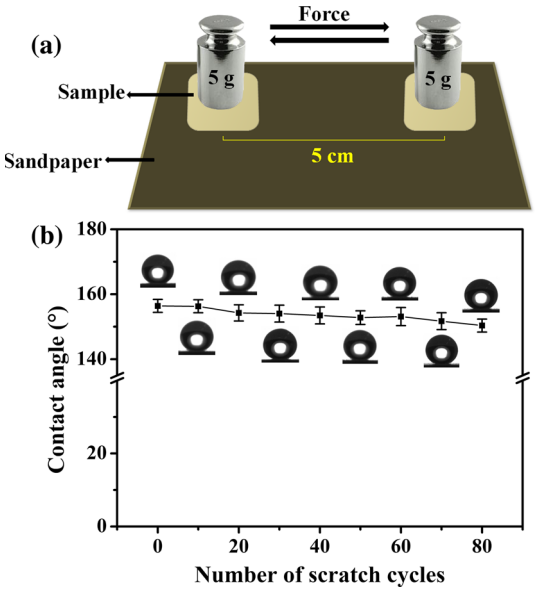

Fig. 6 **a** Schematic illustration of the scratch test. **b** The variation in water CAs on the as-prepared superhydrophobic surface scratched by the sandpaper

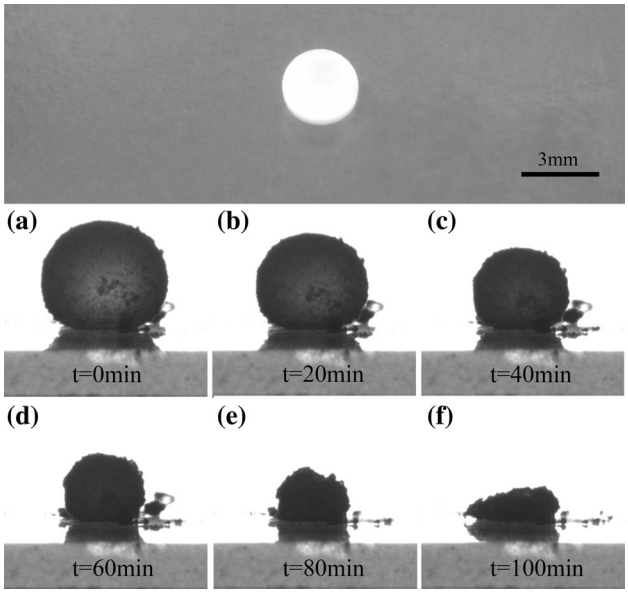

Fig. 8 Horizontal profiles of the same silica liquid marble during evaporation with time obtained by contact angle measurement system video camera

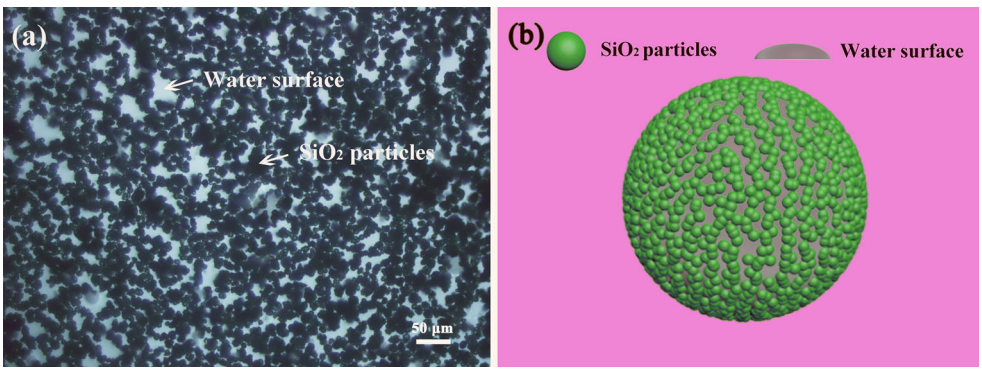

Fig. 7 **a** Surface of the liquid marble coated with silica grains as seen with a microscope, **b** Schematic diagram of the liquid marble

evaporated completely from the structure and the marble finally collapsed.

4 Conclusion

In summary, we have demonstrated a facile one-step spray method to fabricate superhydrophobic coatings by spraying the hydrophobic silica onto the Al substrate. Meanwhile, the corrosion resistance of superhydrophobic coatings was tested in a 3.5 wt% NaCl aqueous solution by way of electrochemistry. The results from polarization curves and EIS demonstrate that the silica coatings provide excellent anticorrosive properties. The superhydrophobic surface also has an excellent function of self-cleaning. In addition, liquid marbles coated with hydrophobic silica nanoparticles were fabricated by rolling the water on the powder beds of hydrophobic silica nanoparticles. Furthermore, the volatility of liquid marbles also was observed.

Acknowledgments The work is supported by the National Natural Science Foundation of China (Grants 21301141 and 21261021) and the Nature Science Foundation of Gansu Province, China (Grant 145RJYA241).

References

1. Barthlott W, Neinhuis C (1997) Planta 202:1
2. Li J, Liu XH, Ye YP, Zhou HD, Chen JM (2011) J Phys Chem C 115:4726
3. Liu S, Liu X, Latthe SS, Gao L, An S, Yoon SS, Liu B, Xing R (2015) Appl Surf Sci 351:897
4. Fj W, Yu S, Ou JF, Li W (2015) J Sol–Gel. Sci Technol 75:625
5. Li J, Yan L, Ouyang Q, Zha F, Jing Z, Li X, Lei ZQ (2014) Chem Eng J 246:238
6. Feng LB, Zhao LB, Qiang XH, Liu YH, Sun ZQ, Wang B (2015) J Sol–Gel Sci Technol 119:75
7. Li J, Li DM, Yang YX, Li JP, Zha F, Lei ZQ (2016) Green Chem 18:541
8. Guo P, Zhai SR, Xiao ZY, Zhang F, An QD, Song XW (2014) J Sol–Gel Sci Technol 72:385
9. Li J, Kang RM, Tang XH, She HD, Yang YX, Zha F (2016) Nanoscale 8:7638
10. Li J, Jing ZJ, Zha F, Yang Y, Wang QT, Lei ZQ (2014) ACS Appl Mater Inter 6:8868
11. Zhang DW, Wang LT, Qian HC, Li XG (2016) J Coat Technol Res 13:11
12. Liu L, Xu F, Ma L (2012) J Phys Chem C 116:18722
13. Zhang F, Chen S, Dong L, Lei Y, Liu T, Yin Y (2011) Appl Surf Sci 257:2587
14. Esmailzadeh S, Khorsand S, Raeissi K, Ashrafizadeh F (2015) Surf Coat Technol 283:337
15. Li J, Jing ZJ, Yang Y, Zha F, Yan L, Lei ZQ (2014) Appl Surf Sci 289:1
16. Li J, Yan L, Li H, Li W, Zha F, Lei ZQ (2015) J Mater Chem A 3:14696
17. Izquierdo A, Ono SS, Voegel JC, Schaaf P, Decher G (2005) Langmuir 21:7558
18. Li J, Wan HQ, Ye YP, Zhou HD, Chen JM (2012) Appl Surf Sci 261:470
19. Liu F, Wang SL, Zhang M, Ma ML, Wang CY (2013) Appl Surf Sci 280:686
20. Ke QP, Fu WQ, Jin HL, Zhang L, Tang TD, Zhang JF (2011) Surf Coat Tech 205:4910
21. Zang D, Liu F, Zhang M, Niu XG, Gao ZX (2015) Chem Eng J 262:210
22. Aussillous P, Quéré D (2001) Nature 411:924
23. Forny L, Pezron I, Saleh K, Guigon P, Komunjer L (2007) Powder Technol 171:15
24. Xue Y, Wang H, Zhao Y, Dai L, Feng L, Wang X (2010) Adv Mater 22:4814
25. Bormashenko E, Musin A (2009) Appl Surf Sci 255:6429
26. Tian J, Arbatan T, Li X, Shen W (2010) Chem Commun 46:4734
27. Glass P, Chung HY, Washburn NR, Sitti M (2010) Langmuir 26:357
28. Allara DL, Parikh AN, Rondelez F (1995) Langmuir 11:2357
29. Stöber W, Fink A, Bohn E (1968) J Colloid Interface Sci 26:62
30. Li J, Wu R, Jing ZJ, Yan L, Zha F, Lei ZQ (2015) Langmuir 31:10702
31. Liu L, Chen R, Liu W, Zhang Y, Shi X, Pan Q (2015) Surf Coat Technol 272:221
32. Li XM, Reinhoudt D, Crego-calama D (2007) Chem Soc Rev 36:1350
33. Roach P, Shirtcliffe NJ, Newton M (2008) Soft Matter 4:224
34. Zhang F, Chen S, Dong L, Lei Y, Liu T, Yin Y (2011) Appl Surf Sci 257:2587
35. Fan Y, Chen Z, Liang J, Wang Y, Chen H (2014) Surf Coat Technol 244:1
36. Liu H, Szunerits S, Xu W, Boukherroub R (2009) ACS Appl Mater Inter 1:1150
37. Xu W, Song J, Sun J, Lu Y, Yu Z (2011) ACS Appl Mater Inter 3:4404
38. Wu LK, Zhang XF, Hu JM (2014) Corros Sci 85:482
39. Zhang F, Zhao L, Chen H, Xu S, Evans DG, Duan X (2008) Angew Chem Int Edit 47:2466
40. Guo Z, Liu W, Su BL (2011) J Colloid Interf Sci 353:335
41. Li J, Yan L, Zhao Y, Zha F, Wang Q, Lei ZQ (2015) Phys Chem Chem Phys 17:6451
42. She Z, Li Q, Wang Z, Li L, Chen F, Zhou J (2013) Chem Eng J 228:415
43. McHale G, Herbertson DL, Elliott SJ, Shirtcliffe NJ, Newton MI (2007) Langmuir 23:918